Field Dependence of Mobilities for Gas-Phase-Protonated Monomers and Proton-Bound Dimers of Ketones by Planar Field Asymmetric Waveform Ion Mobility Spectrometer (PFAIMS)

E. Krylov, E. G. Nazarov, R. A. Miller,† B. Tadjikov, and G. A. Eiceman*

Department of Chemistry and Biochemistry, New Mexico State University, Las Cruces, New Mexico 88003, and SIONEX Corporation, Wellesley Hills, Massachusetts 02481

Received: January 8, 2002; In Final Form: March 19, 2002

The dependence of the mobilities of gas-phase ions on electric fields from 0 to 90 Td at ambient pressure was determined for protonated monomers [$(MH^+(H_2O)_n$] and proton bound dimers [$M_2H^+(H_2O)_n$] for a homologous series of normal ketones, from acetone to decanone (M = C_3H_6O to $C_{10}H_{20}O$). This dependence was measured as the normalized function of mobility $\alpha(E/N)$ using a planar field asymmetric waveform ion mobility spectrometer (PFAIMS) and the ions were mass-identified using a PFAIMS drift tube coupled to a tandem mass spectrometer. Methods are described to obtain $\alpha(E/N)$ from the measurements of compensation voltage versus amplitude of an asymmetric waveform of any shape. Slopes of α for MH^+ versus E/N were monotonic from 0 to 90 Td for acetone, butanone, and pentanone. Plots for ketones from hexanone to octanone exhibited plateaus at high fields. Nonanone and decanone showed plots with an inversion of slope above 70 Td. Proton bound dimers for ketones with carbon numbers greater than five exhibited slopes for α versus E/N, which decreased continuously with increasing E/N. These findings are the first alpha values for ions from a homologous series under atmosphere pressure and are preliminary to explanations of $\alpha(E/N)$ with ion structure.

Introduction

The motion of gas-phase ions in electric fields at pressures greater than 1 Torr has been explored for over a century[1−3] and velocities of ion swarms in controlled atmospheres of drift tubes have been used since the 1960s to model interactions between ions and molecules.[4−7] In recent years, these principles have been developed in mobility spectrometers for the detection of chemical warfare agents and explosives.[8] In general, ion motion is measured as velocity (v_d, cm/s) in uniform gradients of electric fields (E, V/cm) low enough so that velocity is proportional to the electric field through a constant, the coefficient of mobility (i.e., $K = v_d/E$, cm^2/Vs). One relationship between the mobility coefficient, ion structure, and the gas atmosphere is eq 1:[5]

$$K = \frac{3e}{16N}\sqrt{\frac{2\pi}{\mu k T_{\text{eff}}}}\frac{1}{\Omega^{1.1}(T_{\text{eff}})} \qquad (1)$$

where the terms are e, elementary charge; N, drift gas density; μ, reduced ion/neutral mass; T_{eff}, effective temperature of the ion; and Ω, collisional cross section.

The mobility coefficient is characteristic of the structure of an ion and the ion−molecule interactions in a gas; also, K is influenced by collision frequency and energy obtained from the field by ions between collisions. The average energy acquired from the electric field is determined by E/N and is considered negligible when E/N is small since any energy gained by the ion from the field is dissipated at high pressures by collisions with the supporting gas. Under such conditions, K is a constant and independent of E/N. However, the mobility coefficient becomes dependent on electric field with increasing values of E/N as shown in eq 2:[5,7,9]

$$K(E/N) = K(0)[1 + \alpha_2(E/N)^2 + \alpha_4(E/N)^4 + ...] \qquad (2)$$

where terms are $K(0)$, the mobility coefficient under low field conditions and α_2, α_4, ..., α_{2n}, specific coefficients of even powers of the electric field; E/N is in units of Td (under normal conditions 1 Td corresponds to 268.67 V/cm since $E = N_0 10^{-17}$, where N_0 is Loschmidt's constant). The mobility coefficient should be expressed as an even power series in E/N due to symmetry considerations (i.e., the absolute value for ion velocity is independent of electric field direction). When experimental conditions are constant, unique patterns for K versus E/N exist for different ions due to characteristic values of α_{2n}. A simplification of eq 2 has been described[10] where an alpha function is used for the electric field dependence of the coefficient of mobility per eq 3:

$$K(E/N) = K(0)[1 + \alpha(E/N)] \qquad (3)$$

where $\alpha(E/N) = \alpha_2(E/N)^2 + \alpha_4(E/N)^4 + ...$ This formula is a function showing the nonlinear electric field dependence of mobility for specific ions.

Extensive experimental findings exist for the nonlinear dependence of the mobility coefficient on electric field though studies were restricted to simple ions or ions containing only a few atoms. Results available in the Atomic Data of Nuclear Data Tables show that K_o is a nonlinear function with increasing E/N at subambient pressures.[11−14] Comparable findings at ambient pressure (high neutral gas density), where ion−neutral processes exert a dominant role in forming mobility spectra, are not generally available. Only a few studies for the measurement of $K(E/N)$ at ambient pressure have been made owing to

† SIONEX Corporation.

10.1021/jp020009i CCC: $22.00
Published on Web 05/14/2002

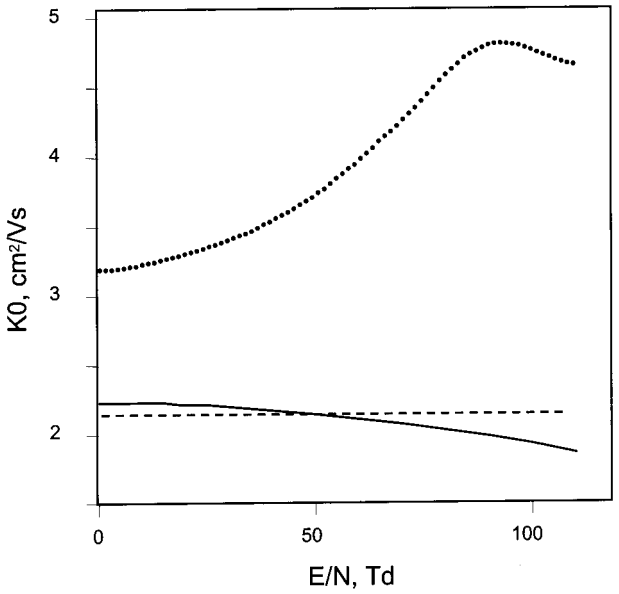

Figure 1. Electric field dependence of the coefficient of mobility for small ions. Plots are for O^- (solid circles), O_2^+ (solid line), and O_2^- (dashed line).

the technical difficulties associated with creating high fields with conventional time-of-flight drift tubes.[15] For example, an electric field of 21360V/cm would be needed to attain values of $E/N \sim$ 80 Td at ambient pressure; this would require a power supply of 106.8 kV for studies with a 5 cm long drift tube. In work presented below, the high field dependence of organic ions with molar masses of 50−250 amu was determined using a planar drift tube operated in air at ambient pressure with asymmetric electric fields. The method of high field asymmetric ion mobility spectrometry is a relatively new technique for ion separations based on a nonlinear, high field dependence for mobility coefficients. The method was proposed in 1982[16] and experimentally demonstrated in 1991−1993.[10,17] Separations were achieved through differences in coefficients for α_n; however, experimental findings lacked a supporting partwork to interpret or analyze the spectra from the perspective of molecular structure. Even today, alpha parameters for atmosphere pressure conditions are available for only a few substances such as amines,[10] chloride,[18] and positive and negative amino acids ions.[19]

In this work, the instrumentation and methods to determine the alpha parameters of large organic ions are described in detail and applied in a systematic investigation for product ions formed from homologous series of ketones. These determinations are made by extracting the values for α_{2n} from the plots of compensation voltage versus separation voltage obtained from the amplitude of the applied waveform. In addition, alpha parameters are reported for individual ions which were mass-identified as protonated monomers and proton bound dimers. Such a systematic investigation should enable the creation of predictive models to relate α_{2n} coefficients to ion structure and molecular properties. This work also establishes the protocol to characterize ion behavior in high fields independent of drift tube design and the protocol was validated using results from reference data.

Analysis of Applied Waveforms and Determination of Field-Dependent Mobilities

General Principles. In Figure 1, an alpha function plot is shown for the electric field dependence of the coefficient of mobility for diatomic ions with positive (O_2^+), negative (O_2^-)

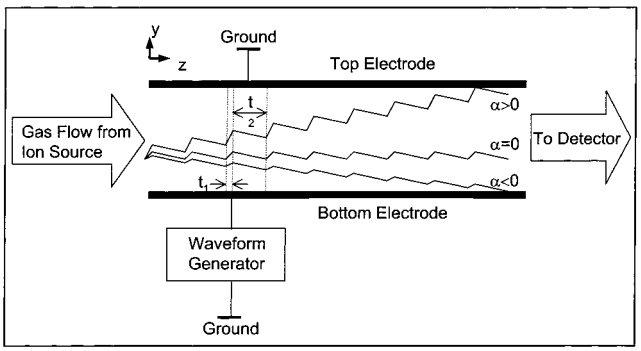

Figure 2. Principle of ions separation in planar field asymmetric ion mobility spectrometry (PFAIMS) for ions with characteristic alpha parameters.

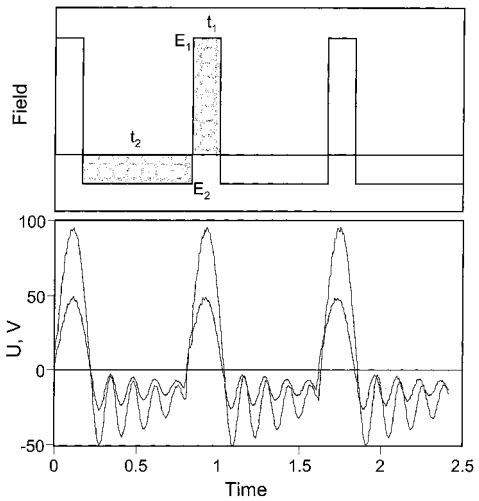

Figure 3. Asymmetric waveform of separation electric field used in PFAIMS drift tube. The waveforms show are theoretical (top part) and actual or experimental (bottom part) used in these experiments.

charge, and a monoatomic ion of negative charge (O^-) in oxygen. This plot, drawn from reference data,[7] illustrates that that mobility coefficients for gas-phase ions in a weak electric field (E/N < 20 Td, i.e., the low field conditions) are constant. However, mobilities can become dependent on E/N at values above 40 Td where $\alpha(E/N) > 0$ for O^- ions, $\alpha(E/N) < 0$ for O_2^+, and $\alpha(E/N) \sim 0$ for O_2^-. These plots and $\alpha(E/N)$ are characteristic of ions and form the basis for ion separation in high field asymmetric waveform ion mobility spectrometry.

In this method for ion separation, ions are introduced in a flow of gas and are carried through a narrow gap between two electrodes as shown in Figure 2. Under the influence of a high frequency, nonsymmetric waveform electric field, applied perpendicular to the direction of gas flow, different species of ions will exhibit characteristic trajectories. For example, an ion under the action of an asymmetric separation field as shown in Figure 3 (top part idealized, bottom part actual measured waveform) will undergo oscillations perpendicular to the gas flow in response to the electric field. This field is designed to satisfied the condition $E_1t_1 = E_2t_2$, i.e., integrals above and below the time axis are equal. If ion mobility does not depend on electric field strength, i.e., $K(E_1) = K(E_2)$, displacement of ions during the high and low portions of the applied field will be equal and opposite (displacement is equal to $v_d\, t_1 = K(E_1)E_1t_1 = -(K(E_2)\, E_2t_2)$. Thus, the sum in displacement of the ions during one period of the separation field will be zero ($K(E_1)$-$E_1t_1 + K(E_2)E_2t_2 = 0$). This case corresponds to low strength field behavior or low mobility dependence $\alpha(E/N) \sim 0$.

If ion mobility significantly depends on electric field strength (i.e., $K(E_1) \neq K(E_2)$), the displacement of ions during a period of the separation field will be not zero, or ($K(E_1)E_1t_1 + K(E_2)E_2t_2 \neq 0$). The direction of displacement will depend on the sign of mobility dependence $\alpha(E/N)$. If $\alpha(E/N) > 0$, then positive ions will be displaced toward the top electrode at a distance $K(E_1)E_1t_1 + K(E_2)E_2t_2. = \Delta KE_1t_1$. The extent of displacement depends on field amplitude (E_1), field waveform (ratio t_1/t_2), and ion mobility dependence (ΔK). Ions with negative mobility dependence, $\alpha(E/N) < 0$, will be displaced toward the bottom electrode.

Ions will pass through the gap between the electrodes only when the net displacement per period of asymmetric field is zero; in contrast, ions that undergo a net displacement will eventually undergo neutralization on one of the electrodes. A displaced ion can be restored to the center of the gap (i.e. compensated, with no net displacement for that ion) when a low strength DC electric field (the compensation field, C) is superimposed on the asymmetric waveform. Ions with differing displacement (owing to characteristic dependence of mobility in the high field condition) can be passed through the gap at compensation fields characteristic of each particular ion and this is accomplished by applying various strengths of C. In this case, this system can function as continuous ion filter; or a scan of C will allow a complete measure of ion species in the analyzer. This resultant scan of C with time will be referred to as mobility scan.

Mathematical Description. A brief mathematical description of the method is presented below and a comprehensive treatment can be found elsewhere.[13] The separation field in a field asymmetric waveform mobility spectrometer, $S(t) = Sf(t)$, is must satisfy the following conditions:

$$1/T\int_0^T S(t)dt \equiv \langle S(t)\rangle = \langle Sf(t)\rangle = S\langle f(t)\rangle = 0 \qquad (4a)$$

$$\langle f^{2n+1}(t)\rangle \neq 0 \qquad (4b)$$

where terms are $f(t)$, a normalized function which describes the waveform; S, the maximum amplitude of the waveform; and $1/T$, the period of the waveform. Triangular brackets in the equations denote the averaging over the period of the separation waveform. The waveform is designed such that the average period value is zero (eq 4a) while the amplitude of positive portion is not equal to negative (asymmetry condition, eq 4b). The addition of the compensation field, C, to the waveform $S(t)$ yields eq 5:

$$E(t) = S(t) + C = Sf(t) + C \qquad (5)$$

so the average ion velocity over a period of the asymmetric waveform can be written as

$$V = \langle V(t)\rangle = \langle K(E)E(t)\rangle \qquad (6)$$

Only ions with average velocity of zero, $\langle V(t)\rangle = 0$, will pass through the gap without neutralization. An expression for the compensation field required to enable an ion to pass through the gap can be obtained by substituting eqs 2−5 into eq 6 as shown here:[10]

$$C = \frac{\langle \alpha S(t)\rangle}{1 + \langle \alpha\rangle + \left\langle \frac{d\alpha}{dE} S(t)\right\rangle}. \qquad (7)$$

The value of this compensation electric field can be predicted precisely when the alpha parameter for the ion species, the waveform $f(t)$, and the amplitude of the asymmetric waveform S are known.

Experimental Section

Instrumentation. Studies were completed using planar drift tubes with field asymmetric waveform ion mobility spectrometry (PFAIMS). One PFAIMS drift tube was equipped with a gas chromatographic inlet to obtain mobility scans for studies on field dependence of mobility. A second PFAIMS drift tube was interfaced to a mass spectrometer for identification of the core ions from peaks in mobility scans. The drift tubes in both instruments were identical in size and shape to those already described.[20] A width of 0.5 mm was used for the gap between the electrodes and air at 2 L/min was used for gas flow through the analyzer. Air was provided using a pure air generator (Mode 737, Addco Corp, Miami, FL) and was further purified through beds of activated charcoal and 13× molecular sieve. The ion source was ~1 mCi of ^{63}Ni.

The drift tube was operated using specialized electronics containing an RF waveform generator, a sweeping voltage generator, and an electrometer. The waveform generator was based on a soft-switched, semiresonant circuit that incorporated a flyback transformer[21] and allowed variable amplitude of the asymmetric waveform from 200V to 1100V without altering the waveform shape (i.e., $f(t)$ is constant). The operating frequency of the RF generator was 1.3 MHz. A trace from the actual waveform is shown in Figure 3 (bottom part) where $f(t)$ is constant though the electric field strength could be varied. A compensation voltage ramp was synchronized with the data collection system and provided a scan of compensation voltage from −35 to +10 V at a frequency of 1 Hz. The entire PFAIMS analyzer was housed in an aluminum box approximately 12 × 10 × 5 cm^3. Total power consumption for the PFAIMS was about 8 W at the maximum amplitude 1100V and about 4W at moderate intensities of 900V. Signal was processed using a National Instruments board (model 6024E) to digitize and store spectra for every scan. Custom software was used to display the results as spectra, topographic plots and graphs of ion intensity versus time.

The gas chromatograph was a Hewlett-Packard model 5710 equipped with a splitless injector, a 15 m SP 2300 capillary column (Supelco, Bellefonte, PA), and a PFAIMS drift tube as the detector.[22] The mass spectrometer was a Sciex TAGA 6000 (Toronto, Ontario, Canada) tandem mass spectrometer (MS). When the drift tube was placed against the flange of the MS, a hole in the drift tube was aligned with the pinhole in the flange of the MS. The MS was equipped with an Apple PowerMac 7100/66 computer and API Standard Software, version 2.5.1. While details of this PFAIMS drift tube/MS interface have already been given,[23] refinements were made with miniaturized electronics and mechanics of operation; also, all parts of the instrument were brought under software control so mass spectra could be obtained while scanning the compensation voltage or at a particular compensation voltage only.

Chemicals and Reagents. Eight normal ketones with carbon numbers from three to 10 (i.e., acetone to decanone) were obtained from various manufacturers in highest available purity. Stock solutions were prepared as mixtures of the ketone in methylene chloride by diluting 1 μL of each chemical in 800 μL of solvent. Working solutions were prepared with serial (1:5) dilutions of the stock solution and the concentrations of solutions for most experiments were 2.8 ± 0.1 mg/mL. In the GC/PFAIMS studies, retention times were determined for individual chemicals prior to any studies.

Procedures. In GC/PFAIM studies, 1 μL of sample was injected with a split ratio of 200:1 so that 1.4×10^{-8} grams per ketone were delivered to the PFAIMS drift tube. The oven was programmed from 70 to 170 °C at a rate of 8 °C/min. During sample collection, the PFAIMS analyzer was operated continuously and mobility scans were obtained every second. Since the widths of individual GC peaks were ~8−10 s at base line during an elution profile, 6−10 mobility scans were recorded for each ketone throughout a range of concentrations. Such measurements were repeated for maximum voltages in the asymmetric waveform from 0 to 1050 V.

Ion identification of a peak in a mobility scan was made in PFAIMS-MS experiments by setting the compensation voltage to pass ions from a single mobility peak to the MS. In these measurements, individual neat chemical was placed in a vapor generator and headspace vapors were diluted and split to the PFAIMS drift tube. The vapor generator was a hermetically sealed, glass container (200 mL), which was thermostated in an aluminum block with a Minco CT 137 controller. Glass diffusion tubes or Teflon permeation tubes was placed in the glass container and temperatures ranged from 35 °C for acetone to 80 °C for decanone. All supply lines from the vapor generator to the drift tube were at 60 °C or more to minimize wall-adsorption by vapors. This flow system allowed a constant gas flow to be delivered to the drift tube and permitted changes in vapor concentration by adjusting the ratio of sample to diluent flows or the sample temperature. The diffusion or permeation tubes were weighed over time to determine gravimetrically concentrations in the sample flow (~5 μg/m^3).

Results and Discussion

Ion Identifications in Planar Field Asymmetric Ion Mobility Spectrometry of Ketones. The ions from a ^{63}Ni source in a PFAIMS drift tube in the absence of ketones appeared at compensation voltage of −9.5V with *m*/*z* values of 19, 37, 55, and 73 amu. These were identified as $(H_3O)^+(H_2O)_n$ where $n = 0-3$ at ambient temperature and moisture of ~1 mg/m^3. Though the identification of the core ion (i.e., a hydrated proton) can be considered reliable, uncertainty exists in the exact composition of the ion population from clustering and declustering in the interface region between ambient pressure and high vacuum. Thus, the factional composition of ions for values of n may not be quantitative derived from intensities in mass spectra. The mass spectra also cannot accurately account for short-lived ion clusters such as $(H_3O)^+(H_2O)_n(N_2)_n$ which also are altered in the supersonic jet expansion region of the IMS/MS. Thus, mass spectra from this experiment are suitable for qualitative interpretations and assignment of identity for the core ion. Nonetheless, the ion chemistry of positive polarity ions in clean air at ambient pressure is well-studied and these results are consistent with such prior findings.[24,25]

When ketone vapors were added to the drift tube, the intensity of peak for $(H_3O)^+(H_2O)_n(N_2)_n$ declined (see Figure 4, bottom part) and two other peaks appeared in the mobility scans. These peaks were at compensation voltages of −3 and +2 V as shown for octanone in Figure 4. The intensity of these new peaks was dependent upon vapor concentration and the compensation voltages were not measurably affected by changes in concentrations over a limited range from the detection limit to the working value. When the compensation voltage was tuned to −3 V, the mass spectrum was found to contain a single peak as shown for octanone in the upper mass spectrum in Figure 4, top part. In this instance, the ion at $m/z = 129$ amu was the protonated monomer of octanone (i.e., $MH^+ (H_2O)_n$ where $M = C_8H_{16}O$ and $n = 0$); a small amount of a hydrated protonated monomer ($n = 1$) is also evident in the mass spectrum. The other ion peak for octanone ($C = +2$ V) yielded a mass spectrum shown in the lower mass spectrum of Figure 4 (top part). This mass spectrum exhibited the same ion as before, $m/z = 129$ amu and an additional peak with *m*/*z* of 257 amu. This other ion is the proton bound dimer of octanone, $M_2H^+ (H_2O)_n$ where $n = 0$ and the peak with *m*/*z* of 129 amu was understood as the product of declustering of the proton bound dimer in the interface between ambient pressure and high vacuum (2×10^{-6} Torr). Decreasing the potential of the orifice, which is known to affect ion fragmentation and declustering in this type of mass spectrometer, tested and confirmed this conjecture. The intensity of the peak for *m*/*z* of 259 amu was increased relative to that for *m*/*z* of 129 amu as the orifice potential was lowered. No other ions of significant intensity were observed and the core ion was assigned to a proton bound dimer.

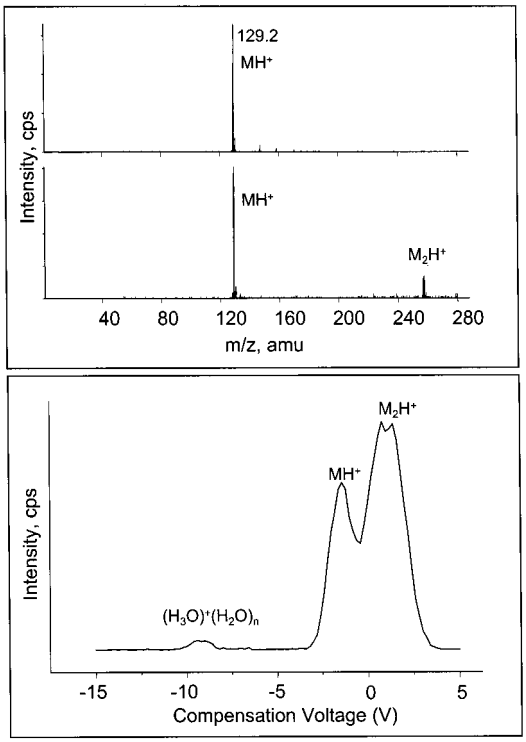

Figure 4. Mass spectra (top part) and mobility scan (bottom part) from octanone in the PFAIMS drift tube coupled to a mass spectrometer.

The identities of peaks in all mobility scans for the other ketones were determined by PFIMS/MS and were found to be protonated monomers and proton bound dimers with minor amounts of core ions with waters of hydration. Two additional examples of mass spectra are shown in Figure 5 for acetone and heptanone.

Mobility Scans for Ketones. All experiments to obtain mobility scans for ketones were made using a gas chromatograph-PFAIMS drift tube in order to eliminate or minimize the possible complications from impurities in samples. Such impurities can alter the observed gas-phase chemistry and the use of prefractionation was useful in maintaining a link between sample purity and spectral integrity. Each experiment was made using mixtures of all ketones and the results from such an experiment are shown in Figure 6. The gas chromatograms shown in the left part was obtained from the sum of all ion current from protonated monomer and proton bound dimers (as marked) and the mobility scans are shown as topographic plots in the right part. As expected for a homologous series, retention times

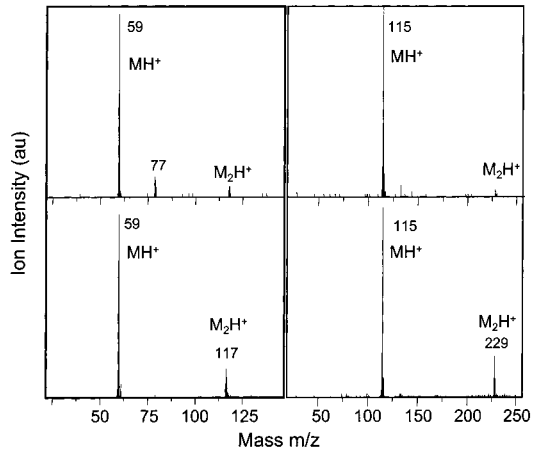

Figure 5. Mass spectra for acetone (left part) and heptanone (right part) for different peaks in the mobility scan from the PFAIMS drift tube-mass spectrometer.

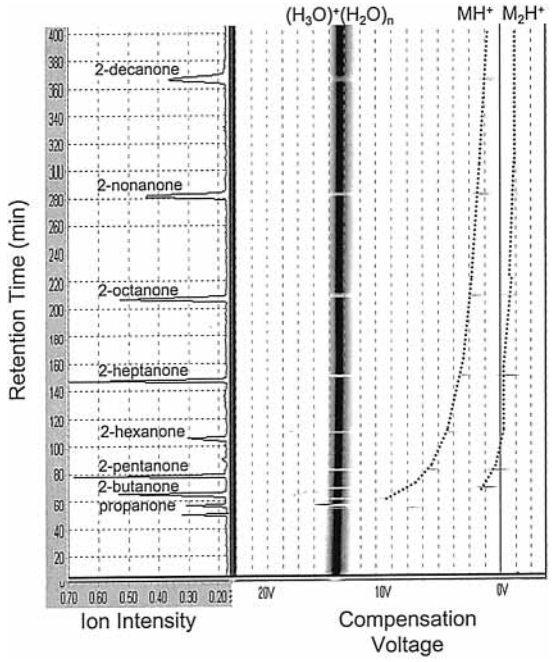

Figure 6. Two-dimensional response of mobility scans (right part) and chromatogram (left part) from GC/PFAIMS experiments for mixture of ketones from acetone to nonanone.

increased with molar mass of the ketone. Significantly, there were no detectable levels of impurities that might interfere with the ion identities and the determination of the alpha functions.

The influence of separation voltage amplitude (*S*) on compensation voltage (*C*) is dependent on the alpha parameter for an ion (see eq 7) and the experimental dependence *C*(*S*) for ketones is shown in Figure 7 for protonated monomers (top part) and proton bound dimers (bottom part). Increased electric field strength in the asymmetric waveform, resulted in increasing negative voltage to restore the transport of protonated monomers through the drift tube. This polarity is consistent with ions that exhibit increased mobilities with increased field strengths and *C* ranged from ~0 V to nearly −15.0 V for acetone at *S* ~1100 V. The absolute magnitude of this change increased inversely with mass: compensation voltages were strongly negative for ions of small molar mass and less so as molar masses increased. Plots for protonated monomers of acetone, butanone, and pentanone ions increased monotonically with increasing electric field, plots for hexanone, heptanone and octanone approached

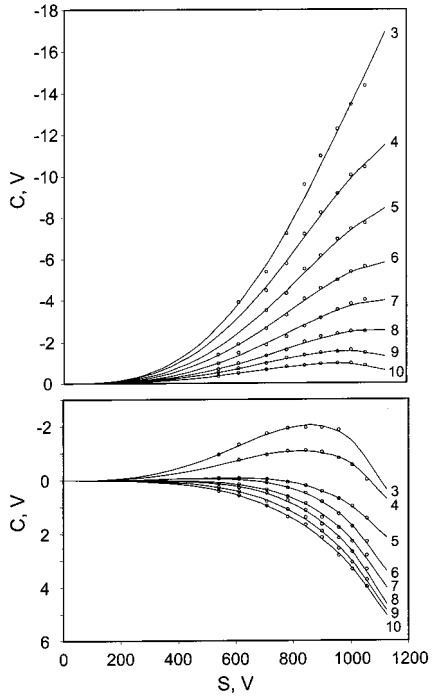

Figure 7. Plots of compensation voltage (*C*) versus amplitude of separation voltage (*S*) for protonated monomers (top part) and proton bound dimers (bottom part) for ketones. Carbon numbers are shown on curves for individual ketone.

plateaus above 1000 V, and plots for nonanone and decanone exhibited a nonmonotonic dependence above 900 V.

The pattern of dependence of C on S for proton bound dimers occurred on a narrow scale compared to protonated monomers with changes spanning ~6.0 V (−2.0 V for acetone at 900 V to +5.0 V for decanone at ~1100 V). Nonetheless, the trend seen above with protonated monomers seemed to continue with the proton bound dimers when viewed as total mass of the ion. Plots for the ions for acetone and butanone exhibit slightly negative slopes, which invert above 900 V. However, plots for proton bound dimers of pentanone to nonanone exhibit plots with continuous and growing slopes toward positive voltage. This means that the mobilities for the proton bound dimers of pentanone to decanone are decreased with increased field strength. These findings are best treated in terms that are independent of the drift tube dimensions and the preference method is to express these findings in alpha parameters. However, field strengths must be extracted from asymmetric waveform and the quality of the waveform for the planar FAIMS drift tube and methods to treat the signal are described in the next section.

Extraction of Alpha Parameters through Processed Asymmetric Waveforms. The procedure of extraction of $\alpha(E/N)$ from experimental measurements of the electric field dependence of the mobility scans has been described.[10,18,19] In this section, some additional considerations regarding the alpha parameter and methods to determine this parameter are described. An important distinction is that the alpha parameter is a function (not a number) and the physical and chemical information about an ion is contained in the shape of the $\alpha(E/N)$ curve. The method of presenting this curve is incidental to the topic. The only criterion critical in these methods is that the calculated values for mobility (i.e., $K(E/N) = K_o(1+\alpha(E/N))$) should be as close as possible to the experimental values. The function for $\alpha(E/N)$ can be represented as an even power series in E/N according McDaniel[7] or as complex form.[18] In both instance, the curves of experimental and calculated results should agree

closely. Thus, the quality of the approximation is limited by the accuracy of the experimental results as already demonstrated.[18] Two parameters were used in these studies and all approximations were located within the error of ΔC (~10%).

In this work, a simple uniform method is described to represent the function of $\alpha(E/N)$, which will be suitable for comparison of results obtained under different experimental conditions. These methods could be used for different asymmetric waveforms or different designs of IMS drift tubes whether linear, cylindrical, or planar FAIMS. The criterion for choosing the level of approximation of alpha is principally to ensure that the method of extracting the alpha parameter involved the fewest individual parameters of the experimental device. Also, the result should contain the fewest adjustable parameters and the approximated curve should be within the experimental error bars. In the next section, details are given for a general method to extract the alpha parameter from experimental findings of C versus S.

The function of $\alpha(E)$ can be given as a polynomial expansion into a series of electric field strength E degrees as shown in eq 8:

$$\alpha(E) = \sum_{n=1}^{\infty} \alpha_{2n} E^{2n} \tag{8}$$

Substituting eq 8 into eq 7 provides a value of the compensation voltage as shown in eq 9 where an uneven polynomial function is divided by an even polynomial function. Therefore, an odd degree polynomial is placed after the identity sign to approximate experimental results:

$$C = \frac{\sum_{n=1}^{\infty} \alpha_{2n} S^{2n+1} \langle f^{2n+1}(t) \rangle}{1 + \sum_{n=1}^{\infty} (2n+1) \alpha_{2n} S^{2n} \langle f^{2n}(t) \rangle} \equiv \sum_{n=1}^{\infty} c_{2n+1} S^{2n+1} \langle f^{2n+1} \rangle \tag{9}$$

This allows the comparison of the expected coefficient (approximated) and values of alpha parameter as shown in eq 10:

$$c_{2n+1} = \alpha_{2n} \langle f^{2n+1} \rangle - \sum_{k=1}^{n-1} (2(n-k)+1) c_{2k+1} \alpha_{2(n-k)} \langle f^{2(n-k)} \rangle \tag{10}$$

Alternatively, alpha parameters can be calculated by inverting the formula using an approximation of the experimental results per eq 11:

$$\alpha_{2n} = \frac{1}{\langle f^{2n+1} \rangle} \{ c_{2n+1} + \sum_{k=1}^{n-1} (2(n-k)+1) c_{2k+1} \alpha_{2(n-k)} \langle f^{2(n-k)} \rangle \} \tag{11}$$

Any number of polynomial terms (e.g., $2n$), in principle, can be determined from eq 11 though a practical limit exists; namely, the number of polynomial terms in the experimental result of the approximation c_{2n+1} should be higher than the expected number of alpha coefficients α_{2n}. Since the size of n depends on the experimental error, the power of the approximation of the experimental curves $C(S)$ cannot be increased without limit. Usually N experimental points of $C_i(S_i)$ exist for the same ion species and experimental data can be approximated by the polynomial using a conventional least-squares method. Finally, increasing the number of series terms above the point where the fitted curves are located within the experimental error bars is unreasonable. In practice, two or three terms are sufficient to provide a good approximation as shown in prior findings.[18]

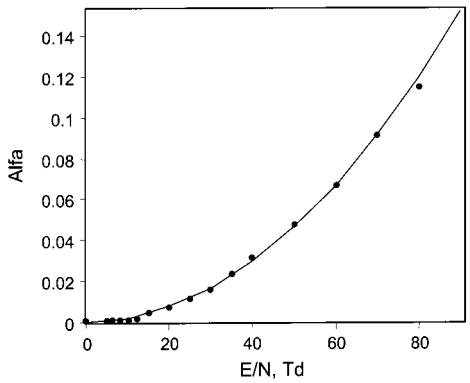

Figure 8. Validation of the method for determining α functions. The solid line is the alpha fuction for O_2^- ions using PFAIMS at ambient pressure and data reduction methods described in this work. The solid circles are points for O_2^- from Atomic Data and Nuclear Data Tables.[14]

The error in measurements must be determined in order to gauge the order of a polynomial for alpha. The sources of error in these experiments (with known or estimated error) were

1. error associated with measurement and modeling of the separation field amplitude (~5%),

2. error in C(S) from a first-order approximation of eq 4 (~3%),

3. Error in measuring the compensation voltage (~2%). The approximate combined error may be ~10% and there is therefore no gain with approximations beyond two polynomial terms; thus, alpha can be expressed as $\alpha(E/N) = \alpha_2(E/N)^2 + \alpha_4(E/N)^4$ with a level of accuracy as good as permitted by the measurements.

Modern software usually provides the possibility to approximate experimental data by polynomial function $C = c_3S^3 + c_5S^5$ according to eq 9. A standard least-squares method (regression analysis) was used to approximate or model the experimental findings. For N experimental points with $C_i(S_i)$ and for $C = c_3S^3 + c_5S^5$ a function $y = c_3 + c_5x$ can be defined where $y = C/S^3$; $x = S^2$ so c_5 and c_3 are given by eqs 12 and 13, respectively:

$$c_5 = \frac{\sum_{i=1}^{N} x_i \sum_{i=1}^{N} y_i - N \sum_{i=1}^{N} x_i y_i}{(\sum_{i=1}^{N} x_i)^2 - N \sum_{i=1}^{N} x_i} \tag{12}$$

$$c_3 = \frac{1}{N} (\sum_{i=1}^{N} y_i - c_5 \sum_{i=1}^{N} x_i) \tag{13}$$

Through substituting experimental values for c_3 and c_5, the derived values for α_2 and α_4 can be found per eqs 14 and 15:

$$\alpha_2 = \frac{c_3}{\langle f^3 \rangle} \tag{14}$$

$$\alpha_4 = \frac{c_5 + 3c_3\alpha_2\langle f^2 \rangle}{\langle f^5 \rangle} \tag{15}$$

This formula is valid for any waveform and may be described by form factors $\langle f^2(t) \rangle$ $\langle f^3(t) \rangle$ $\langle f^5(t) \rangle$; these can be calculated

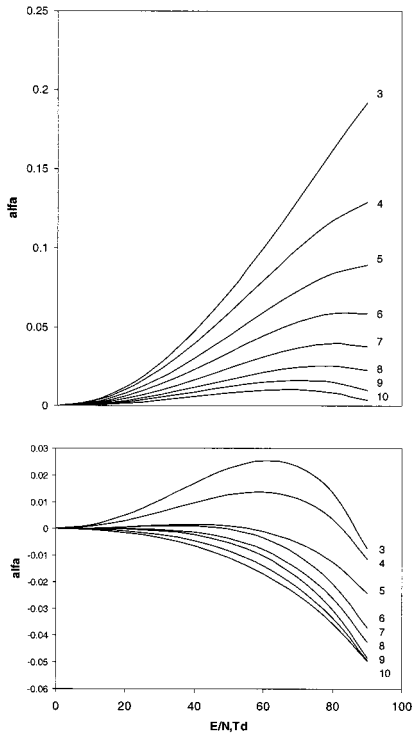

Figure 9. Plots of $\alpha(E/N)$ for ketones for protonated monomers (top part) and proton bound dimers (bottom part). Carbon numbers for individual ketones are labeled.

analytically or numerically. In an alternate approach that was not employed in this work, harmonic approximation functions of real waveform may be used in the computations of α dependence.[18] An actual asymmetry waveform may have a complex character as can be seen in Figure 3 (bottom part) and second, third, and fifth orders in the equations will be needed to determine $\alpha(E/N)$; any errors in these parameters will increase errors in the value of the alpha parameter. Therefore, numerical computation of the real waveform was used to obtain accurate values of form factors $\langle f^2(t)\rangle$ $\langle f^3(t)\rangle$ $\langle f^5(t)\rangle$. For the actual waveform shown in Figure 3, the real field form factors were determined as $\langle f^2\rangle = 0.187066$, $\langle f^3\rangle = 0.093339$, and $\langle f^5\rangle = 0.08477721$. However, validation of this approach was needed.

To verify eqs 14 and 15, control experiments were made using the PFAIMS with simple O_2^- ions in dry (0.1 ppm moisture) air. In this experiment, the parameter E/N was changed from 0 to 80 Td at atmosphere pressure and room temperature $T = 25$ °C. A comparison was made between the experimentally determined alpha function for O_2^- ions (solid line in Figure 8, from actual parameters for the form factors of the real waveform in Figure 3, bottom part) and values for $\alpha(E/N) = [K(E/N) - K(0)]/K(0)$ obtained from Atomic Data and Nuclear Data tables for O_2^- ions in low-pressure conditions (page 84 in ref 14). The reference data values are shown as symbols in Figure 8 and the favorable agreement between the reference values and results from this method is a direct validation of the instrumentation and procedures to derive alpha parameters as described in this work.

Alpha Functions for Ketones. The final result from these efforts are shown in Figure 9 as plots of the function for $\alpha(E/N)$ for individual ketones spanning electric fields of 0 to 80 Td and in Table 1. These plots are fundamental features of ions that are independent of the drift tube parameters and could be used in other mobility spectrometers. These results are surprising and demonstrate that chemicals with the same functional group, protonated monomers of a single type, can exhibit a broad range of behavior vis-à-vis the dependence of coefficients of mobility on electric fields.

This difference in behavior for a common moiety suggests that the effect from the electric field must be associated with other aspects of molecular structure. One possible interpretation is that ions are heated during the high field and the effect on the protonated monomer should be striking. These ions with structures of $MH^+(H_2O)_n$ or perhaps $MH^+(H_2O)_n(N_2)_2$, should be prone to dissociation with slight increases in ion temperature caused by the high field conditions.[26] Thus, ions cross-sections and mobilities would accompany declustered small ions at high fields. An example is the 20% increase in $\alpha(E/N)$ for the protonated monomer of acetone with high fields. As the molecular weight of the ketone increases, ion heating should be less pronounced and reflected in the $\alpha(E/N)$ function. The $\alpha(E/N)$ function for proton bound dimers is consistent with decreases in mobility under high field conditions. Consequently, the basis for the $\alpha(E/N)$ function differs from that of protonated monomers. Indeed, the proton bound dimer for decanone undergoes a 5% decrease at high fields. The cause for a decrease in mobility at high fields has no existing model but could be due to increased collisional size or increased strength of interaction between the ion and the supporting gas.

Three final features of these experiments can be observed in Figure 10. The effect of ion mass on $\alpha(E/N)$ is shown regardless of ion formula and is the first presentation of a homologous series in field asymmetric ion mobility spectrometry. The plot shows that the curves can be approximated with a common function though there is no experimental or theoretical background material for such predictions.

The actual values for alpha coefficients are given in Table 1. The accuracy of approximations of error was calculated with a

TABLE 1: Values for Alpha Parameters for Ions of Ketones

	protonated monomer							
	acetone	butanone	pentanone	hexanone	heptanone	octanone	nonanone	decanone
formula	$C_3H_6OH^+$	$C_4H_8OH^+$	$C_5H_{10}OH^+$	$C_6H_{12}OH^+$	$C_7H_{14}OH^+$	$C_8H_{16}OH^+$	$C_9H_{18}OH^+$	$C_{10}H_{20}OH^+$
m/*z*(amu)	59	73	87	101	115	129	143	157
α_2	3.14×10^{-5}	2.7×10^{-5}	2.1×10^{-5}	1.7×10^{-5}	1.2×10^{-5}	8.4×10^{-6}	6.5×10^{-6}	4.6×10^{-6}
α_4	-9.54×10^{-10}	-1.4×10^{-9}	-1.2×10^{-9}	-1.1×10^{-9}	-8.8×10^{-10}	-6.9×10^{-10}	-6.6×10^{-10}	-5.2×10^{-10}
LSD(%)	4.14	1.89	2.4	1.82	4.14	2.23	1.88	2.21
	proton bound dimer							
	acetone	butanone	pentanone	hexanone	heptanone	octanone	nonanone	decanone
formula	$(C_3H_6O)_2H^+$	$(C_4H_8O)_2H^+$	$(C_5H_{10}O)_2H^+$	$(C_6H_{12}O)_2H^+$	$(C_7H_{14}O)_2H^+$	$(C_8H_{16}O)_2H^+$	$(C_9H_{18}O)_2H^+$	$(C_{10}H_{20}O)_2H^+$
m/*z*(amu)	117	145	173	201	229	257	285	303
α_2	1.34×10^{-5}	8.0×10^{-6}	1.9×10^{-6}	1.9×10^{-6}	2.5×10^{-7}	-3.5×10^{-7}	-2.2×10^{-6}	-3.5×10^{-6}
α_4	-1.77×10^{-9}	-6.0×10^{-10}	-8.0×10^{-10}	-6.8×10^{-10}	-6.9×10^{-10}	-4.8×10^{-10}	-3.2×10^{-10}	-1.2×10^{-9}
LSD(%)	2.96	1.23	3.34	3.82	3.48	2.87	2.84	2.15

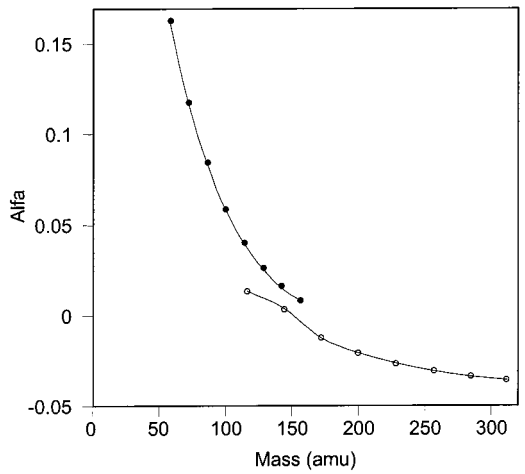

Figure 10. Empirical relationship between α(80 Td) values and ion mass for ketone ions. Symbols are solid circles for protonated monomers and open circles for proton bound dimers.

TABLE 2: Comparison of Compensation Voltages from Actual and Derived Values

S, V	*C*, V exptl	*C*, V theory
782.5	−4.32	−4.455
843.8	−5.49	−5.325
901.3	−6.14	−6.165
960	−6.92	−7.02
1008	−7.44	−7.7
1056	−7.7	−8.375

least-squares deviation (LSD) as $\sqrt{1/N\sum_1^N(R-A)^2/A^2}$ where R is the experimental value and A is the approximated value. Results are shown in Table 1 and the standard deviation for all ions did not exceed 5%. This supports the prior approximations which were based on ∼10% error.

The calculated $\alpha(E/N)$ dependence was used for direct numerical modeling of ion motion to check the validity of suggested method of mobility dependence calculation. The procedure was as follows: the experimental data set for protonated monomer of pentanone was processed to calculate $\alpha(E/N)$ function; the product of the real waveform and the calculated $\alpha(E/N)$ function was numerically integrated to find the ion drift velocity for a certain value of separation voltage; and the corresponding compensation voltage value was calculated. Both calculated and experimental values of compensation voltage are presented in Table 2. Correlation between two sets of data is 0.9885 and further supports the accuracy of these methods.

Conclusion

The fundamental dependence of the mobility of ions in high electric field can be obtained from planar field asymmetric ion mobility spectrometry. Functions of the dependence can be extracted from experiments of compensation voltage with amplitude of separation voltage using methods to treat any imperfect waveforms. Error analysis suggests that the determinations are better than 10%. These findings show an internal consistency for homologues series of ketones and illustrate a previously undisclosed mass dependence of alpha functions for large organic ions.

Acknowledgment. Support is gratefully acknowledged from the university cooperation grants from Charles Stark Draper Laboratory (Award No. DL-H-516600) and from NASA (Grant No. 00-HEDS-01-110). We also acknowledge the helpful suggestions on chemistry and proofing the manuscript from Prof. John Stone, Queen's University, Kingston, Ontario.

Terms and Abbreviations

letter	dimension	name
E	V/cm	electric field
N	cm^{-3}	gas density
v_d, V	cm/s	ion drift velocity
K	cm^2/ V s	ion mobility
K_0	cm^2/ V s	ion mobility in weak electric field
$\alpha(E/N)$	n/d	normalized mobility field dependence
α_2, α_4, α_6 ...	Td^{-2}, Td^{-4}, Td^{-4}, ...	coefficient of $\alpha(E)$ approximation as an even power series in E/N
C	V/cm	compensation field
c_3, c_5, ...	V cm^{-1} Td^{-3}, V cm^{-1} Td^{-5}, ...	coefficient of $C(S)$ approximation as an odd power series in S
S	Td	separation field
$f(t)$	n/d	normalized separation field waveform
$\langle\rangle$		triangular brackets denote the averaging over the period of separation field

References and Notes

(1) Langevin, P. *Ann. Chim. Phys.* **1903**, *28*, 289−384.
(2) Langevin, P. *Ann. Chim. Phys.* **1905**, *8*, 245−288.
(3) Tyndall, A. M. *The Mobility of Positive Ions in Gases*; University Press: Cambridge, England, 1938.
(4) Mason, E. A.; Schamp, H. W., Jr. *Ann. Phys. (NY)* **1958**, *4*, 233.
(5) Mason, E. A.; McDaniel, E. W. *Transport Properties of Ions in Gases*; Wiley: New York, 1988.
(6) Pai, R. Y.; Ellis, H. W.; Akridge, G. R.; McDaniel, E. W. *J. Chem. Phys.* **1976**, *65*(8), 3390−1.
(7) McDaniels, E. W.; Mason, E. A. *The Mobility and Diffusion of Ions in Gases*; Wiley: New York, 1973; pp 266−326.
(8) Ewing, R. G.; Atkinson, D. A.; Eiceman, G. A.; Ewing, G. J. *Talanta* **2001**, *54*, 515−529.
(9) Carr, T. W. *Plasma Chromatography*; Plenum: New York, 1984.
(10) Buryakov, I. A.; Krylov, E. V.; Nazarov, E. G.; Rasulev, U. Kh. *Int. J. Mass Spectrom.* **1993**, *128*, 143−148.
(11) Ellis, H. W.; Pai, R. Y.; McDaniel, E. W.; Mason, E. A.; Viehland, L. A. Transport Properties of Gaseous Ion over a Wide Energy Range. *At. Data Nucl. Data Tables* **1976**, *17*, 177−210.
(12) Ellis, H. W.; McDaniel, E. W.; Albritton, D. L.; Viehland, L. A.; Lin, S. L.; Mason, E. A. Transport Properties of Gaseous Ion over a Wide Energy Range. *At. Data Nucl. Data Tables* **1978**, *22*, 179−217.
(13) Ellis, H. W.; Thackston, M. G.; McDaniel, E. W.; Mason, E. A. Transport Properties of Gaseous Ion over a Wide Energy Range. *At. Data Nucl. Data Tables* **1984**, *31*, 113−151.
(14) Viehland, L. A.; Mason, E. A. Transport Properties of Gaseous Ion over a Wide Energy Range. *At. Data Nucl. Data Tables* **1995**, *60*, 37−95.
(15) Eiceman, G. A.; Karpas, Z. *Ion Mobility Spectrometry*; CRC Press: Boca Raton, FL, 1993; p 112.
(16) Gorshkov, M. P. Invention's Certificate No. 9666583, Russia, G01N27/62, 1982.
(17) Buryakov, I. A.; Makas', A.; Krylov, E. V.; Nazarov, E. G.; Pervukhin, V. V.; Rasulev, U. Kh. *Sov. Technol. Phys. Lett.* **1991**, *17*, 60−65; translation, *Am. Technol. Phys.* **1991**, 446−447.
(18) Viehland, L. A.; Guevremont, R.; Purves, R. W.; Barnett, D. A. *Int. J. Mass Spectrometry* **2000**, *197*, 123.
(19) Guevremont, R.; Barnett, D. A.; Purves, R. W.; Viehland, L. A. *J. Chem. Phys.* **2001**, *14*, 10270−10277.
(20) Miller, R. A.; Eiceman, G. A.; Nazarov, E. G.; King, A. T. *Sens. Actuators, B* **2000**, *67*, 300−306.
(21) Krylov E. V. *Instrum. Exp. Tech.* **1997**, *40*(5) 628−632.
(22) Eiceman, G. A.; Tadjikov, B.; Krylov E. V.; Nazarov, E. G.; Miller, R. A.; Westbrook, J.; Funk, P. *J. Chromatogr. A* **2001**, *917*, 205−217.
(23) Eiceman, G. A.; Nazarov, E. G.; Miller, R. A. *Int. J. Ion Mobility Spectrom.* **2001**, *3*, 15−27.
(24) Kim, S. H.; Betty, K. R.; Karasek, F. W. *Anal. Chem.* **1978**, *50*, 2006−2011.
(25) Ketkar, S. N.; Dheandhanoo, S. *Anal. Chem.* **2001**, *73*, 2554−2558.
(26) Kim, S. H.; Betty, K. R.; Karasek, F. W. *Anal. Chem.* **1978**, *50*, 2006−2011.